INTERFACE

rsif.royalsocietypublishing.org

Research

Cite this article: Stavenga DG, Otto JC, Wilts BD. 2016 Splendid coloration of the peacock spider *Maratus splendens*. *J. R. Soc. Interface* **13**: 20160437.
http://dx.doi.org/10.1098/rsif.2016.0437

Received: 3 June 2016
Accepted: 13 July 2016

Subject Category:
Life Sciences–Physics interface

Subject Areas:
biophysics

Keywords:
ommochromes, iridescence, colour, scattering, opisthosoma, vision

Author for correspondence:
Doekele G. Stavenga
e-mail: d.g.stavenga@rug.nl

Electronic supplementary material is available at http://dx.doi.org/10.1098/rsif.2016.0437 or via http://rsif.royalsocietypublishing.org.

THE ROYAL SOCIETY PUBLISHING

Splendid coloration of the peacock spider *Maratus splendens*

Doekele G. Stavenga[1], Jürgen C. Otto[2] and Bodo D. Wilts[3]

[1]Computational Physics, Zernike Institute for Advanced Materials, University of Groningen, Nijenborgh 4, 9747AG Groningen, The Netherlands
[2]19 Grevillea Avenue, St. Ives, New South Wales 2075, Australia
[3]Adolphe Merkle Institute, University of Fribourg, Chemin des Verdiers 4, 1700 Fribourg, Switzerland

DGS, 0000-0002-2518-6177; BDW, 0000-0002-2727-7128

Jumping spiders are well known for their acute vision and often bright colours. The male peacock spider *Maratus splendens* is richly coloured by scales that cover the body. The colours of the white, cream and red scales, which have an elaborate shape with numerous spines, are pigmentary. Blue scales are unpigmented and have a structural colour, created by an intricate photonic system consisting of two chitinous layers with ridges, separated by an air gap, with on the inner sides of the chitin layers an array of filaments. We have characterized the optical properties of the scales by microspectrophotometry, imaging scatterometry and light and scanning electron microscopy. Optical modelling revealed that the filament array constitutes a novel structural coloration system, which subtly fine tunes the scale reflectance to the observed blue coloration.

1. Introduction

Male jumping spiders of the Australian salticid genus *Maratus* (Karsch 1878) have brightly coloured opisthosomal flaps that are raised and oscillated sideways during their courtship display [1,2]. The genus is accordingly referred to as peacock spiders. The colourful patterns, with often striking contrasts of white, cream, yellow or red versus blue, are owing to scales (modified hairs) that cover the spider's body [3–5]. Visual observations indicate that the cream to red scales are pigmented and that the blue scales are structurally coloured and iridescent [4].

Only a limited number of studies have so far been devoted to the chemical (pigmentary) and physical (structural) basis of spider coloration. Ommochromes have been demonstrated to be the main pigments, and this has been particularly well studied in crab spiders [6–9]. Bile as well as melanin pigments have also been encountered [7,10].

Spiders employ a variety of structural coloration mechanisms [4,11,12]. The cuticle of the jumping spider *Cosmophasis thalassina* acts as a first-order diffraction grating, which together with an underlying broadband multilayer reflector causes distinct iridescence [13]. Similar stacks of chitinous layers with alternating high and low refractive indices, acting as green iridescent reflecting multilayers, were identified in the cuticle of the chelicerae of the tube-web spider *Segestria florentina* and the jumping spider *Phidippus johnsoni* [14,15].

In addition to a coloured cuticle, many spider species have structurally coloured hairs and scales. Lamellated hairs, consisting of chitin and air thin films or quasi-ordered structures, act as blue reflectors in tarantulas, Theraphosidae [4,10,16]. A specifically interesting theraphosid, *Poecilotheria metallica*, features in addition to the blue hairs slightly differently organized, pigmentless hairs, which exhibit a yellow structural colour [4]. The male jumping spider *Cosmophasis umbratica* has two types of iridescent scales with a rather simple architecture [17]. Type I scales consist of two thin chitin layers separated by an air gap, together acting as an ultraviolet and green–orange reflector. These scales play a crucial role in male–male contests [18]. Type II scales similarly have two layers, however closely opposed to each other, causing a purple reflector [17].

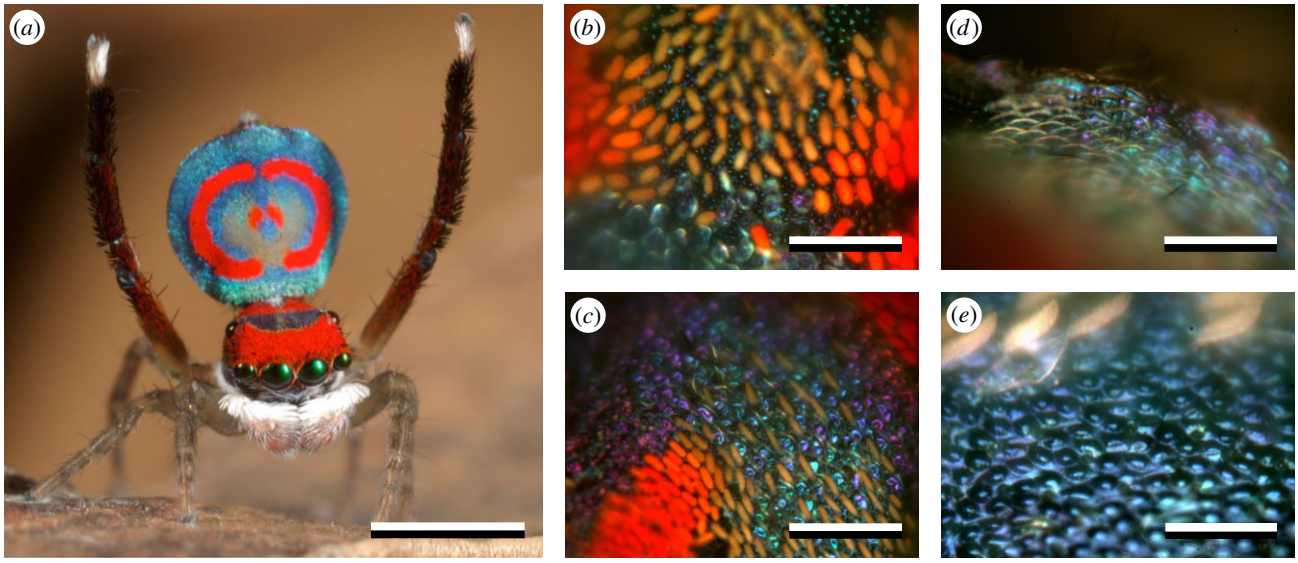

Figure 1. Coloration of the male peacock spider *Maratus splendens*. (*a*) Courting male. (*b*) The central part of the opisthosoma with mainly pigmented scales, coloured red, orange and cream-yellow. (*c*) At other locations blue or purple scales occur. (*d*) The blue scales are distinctly convex. (*e*) The cuticle consists of convex, blue coloured cells. Scale bars, (*a*) 2 mm; (*b–d*) 100 µm; (*e*) 50 µm.

Here, we present an analysis of the various coloration mechanisms applied by one of the most impressively coloured male peacock spiders, appropriately named *Maratus splendens* (Arthropoda: Arachnida: Araneae: Salticidae; figure 1*a*). By using spectrophotometry, imaging scatterometry and scanning electron microscopy, we found that the red and cream to yellow scales of the peacock spiders have a pigmentary colour. The blue scales derive their colour from multilayer reflector properties, however with uniquely structured filaments to fine-tune the spectral reflectance [4,9,17].

2. Material and methods

2.1. Animals

Male *M. splendens* (Rainbow 1896) were locally captured in Lane Cove National Park, Sydney, Australia. Survey images of the scale organization at the opisthosoma were made with an Olympus SZX16 stereomicroscope (Olympus, Tokyo, Japan; figure 1*b–e*). Photographs of single scales, obtained by gently pressing an animal onto a microscope slide (figures 2*a*,*b*, 3*a–d* and 4*a*,*b*), were made with a Zeiss Universal Microscope (Zeiss, Oberkochen, Germany) equipped with an Olympus LUCPlanFL N 20×/0.45 objective.

2.2. Imaging scatterometry

The spatial reflection characteristics of the scales were studied with an imaging scatterometer. A small piece of cuticle with scales attached was glued to the tip of a glass micropipette, thus allowing the scales to be positioned at the first focal point of the ellipsoidal mirror of the scatterometer. Scatterograms (figures 2*d* and 4*c*) were obtained by focusing a white-light beam with a narrow aperture (less than 5°) onto at a small circular area (diameter approx. 13 µm) of a scale, and the spatial distribution of the far-field scattered light was then monitored. A flake of magnesium oxide served as a white diffuse reference object (for further details, see [19]).

2.3. Anatomy

For scanning electron microscopy (figures 2*c*, 3*e*, 4*f*,*g* and 5*a*), the scales were sputtered with a 3 nm thick layer of gold and observed with a MIRA 3 LMH field-emission electron microscope (Tescan, Brno, Czech Republic).

2.4. Spectroscopy

Reflectance spectra of single wing scales *in situ* and of bare cuticle (figures 2*e*, 3*f* and 4*d*) were measured with a microspectrophotometer (MSP), being a Leitz Ortholux microscope (Leitz, Wetzlar, Germany) connected to an AvaSpec 2048-2 CCD detector array spectrometer (Avantes, Eerbeek, The Netherlands), with light supplied by a xenon arc light source. The microscope objective was an Olympus LUCPlanFL N 20×/0.45. A white diffuse reference tile (Avantes WS-2) was used as a reference. Transmittance spectra of single scales, immersed in water and covered with a coverslip, were also measured with the MSP (figures 2*f* and 4*e*).

2.5. Modelling of reflectance spectra

The reflectance spectra of the blue scales were modelled for normally incident light using a matrix transfer formalism [20–22]. We assumed the scales to consist of two solid chitin layers, with thickness d_c, separated by an air layer with thickness d_a. At the outside a ridge layer with thickness d_r exists and the inside has a filament layer with thickness d_f (figure 5). Like the layers, the ridges and filaments were assumed to consist of chitin, the refractive index of which is given by $n_c(\lambda) = A + B/\lambda^2$, with $A = 1.517$ and $B = 8.80 \times 10^3$ nm^2 [23]. We assumed a sinusoidal shape for the ridge cross section and calculated the effective refractive index profile with the height-depending fraction of chitin as the weighting factor between chitin and air. The refractive index thus gradually increased from that of air ($n_a = 1$) to that of chitin. For the filament layer inside the scale, we assumed an effective refractive index $n_f = fn_c + (1 - f)n_a$, where f is the filling factor of the chitinous filament; in the modelling, we used $f = 0.25$.

3. Results

3.1. Appearance of body and scales of *Maratus splendens*

The opisthosomal flaps of male *M. splendens* form during the courtship display two red, symmetrically curved bands,

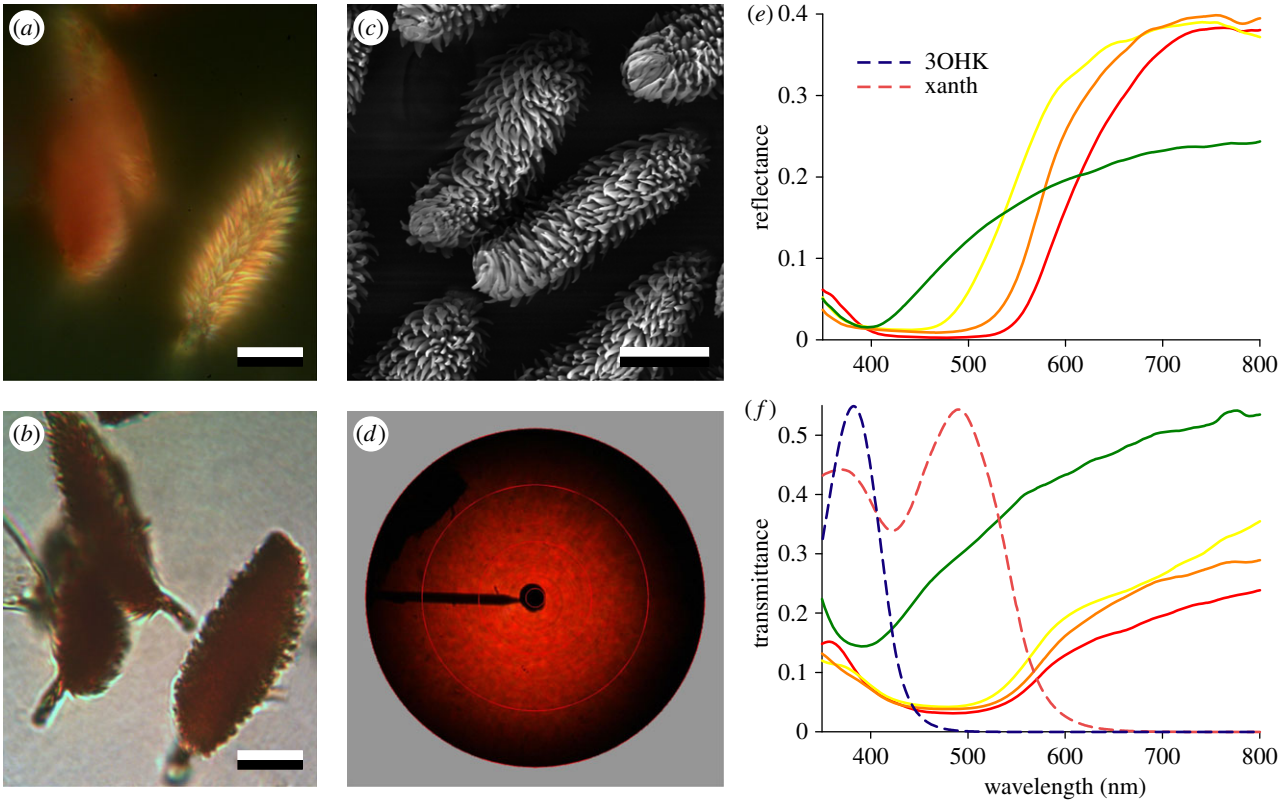

Figure 2. Optical properties of pigmentary coloured scales of *Maratus splendens*. (*a*) Epi-illumination light microscopy of two red scales (left) and a cream-yellow scale (right). The scales have barbs with width approximately 1.5 µm and length approximately 3.5 µm. (*b*) The same scales observed with transmitted light. (*c*) Scanning electron micrograph of pigmented scales. (*d*) Scatterogram of a red scale attached to a piece of cuticle, showing that the pigmented scales reflect very diffusely. The red circles indicate scattering/reflection angles of 5, 30, 60 and 90°, respectively; the black bar at 9 o'clock is due to the glass pipette holding the piece of cuticle (black centre). (*e*) Reflectance spectra measured with an MSP of a cream (green curve), yellow, orange and red scale. (*f*) Transmittance spectra of a cream (green curve), yellow, orange and red scale immersed in water. The size of the measurement area in (*e*) and (*f*) was 5×5 µm^2. The dashed curves are the absorption spectra of 3-OH-kynurenine (3OHK) and xanthommatin (xanth; arbitrary peak value 0.54). Scale bars, (*a*–*c*) 10 µm.

creating together an almost closed red circle, with two central red spots in a main blue field (figure 1*a*). Close inspection showed that the red bands consist of a dense array of scales with colour varying from scarlet-red to cream-yellow (figure 1*b*,*c*). The scales in the adjacent area were blue to purple, depending on the angle of viewing, or elsewhere rather colourless. In grazing view, the blue scales appeared to be convex (figure 1*d*). The scales did not fully cover the cuticle; the latter was seen to consist of slightly convex, hexagonally packed cells with a distinct bluish colour (figure 1*e*). To investigate the origin of the various colours, we performed light and scanning electron microscopy, imaging scatterometry and microspectrophotometry.

3.2. Optics and anatomy of pigmented scales

Light and electron microscopy of the cream-yellow and red scales demonstrated that they are studded with spiny extensions (figure 2*a*–*c*). The irregular structure will predictably widely scatter incident light. Indeed, imaging scatterometry demonstrated that the scales act as a diffusely scattering material (figure 2*d*) [24].

Reflectance spectra measured from individual scales with an MSP yielded a low reflectance at short wavelengths with a strong rise in reflectance at longer wavelengths, characteristic for short-wavelength absorbing material (figure 2*e*). Among the measured spectra, two distinct classes could be distinguished. Yellow–orange to red scales (yellow to red curves in figure 2*e*) had a much steeper slope than cream scales (green curve in figure 2*e*), indicating that at least two different pigments were present.

To characterize the pigments, we measured transmittance spectra on isolated scales, which were immersed in water in order to reduce the light loss created by scattering. In the cream scales, the pigment-induced drop in transmittance was significantly less than that of the yellow–orange to red scales (figure 2*f*). The spectra obtained indicate the presence of different pigments, possibly 3-OH-kynurenine and xanthommatin. For comparison, we include their absorption spectra in figure 2*f* (dashed curves, arbitrarily normalized; taken from fig. 3D of Stavenga *et al.* [24]).

In addition to the distinctly coloured cream to red scales, whitish scales were encountered, of which figure 3 presents two examples. They were observed with epi-illumination (figure 3*a*,*c*) as well as transmitted light (figure 3*b*,*d*) and are shown in perpendicular (figure 3*a*,*b*) and side view (figure 3*c*,*d*), respectively. The images show that the scales are asymmetrical, with a smooth surface facing the cuticle and a forest of protrusions at the scale upper side (figure 3*e*). The rough upper side strongly scatters incident light, causing the white appearance with epi-illumination and the dark features of the transmitted light images, respectively. The white colour suggested the absence of pigment, but reflectance measurements made with the MSP showed a reduced reflectance in the ultraviolet wavelength range, indicative of the presence of trace amounts of 3-OH-kynurenine in the scales (figure 3*f*).

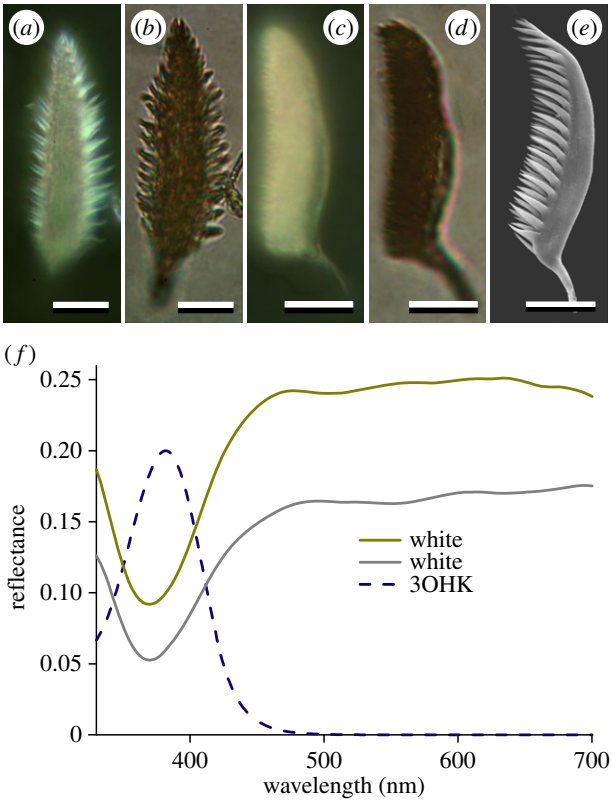

Figure 3. Optical properties of white scales of *Maratus splendens*. (*a*) Epi-illumination light microscopy of a white scale seen from above. (*b*) The same scale with transmission light microscopy. (*c*) Another scale observed with epi-illumination light microscopy. (*d*) The same scale in transmitted light. (*e*) Scanning electron microscopy of a scale in side view. (*f*) Reflectance spectra of two white scales measured with a microspectrophotometer and the absorption spectrum of 3-OH-kynurenine (3OHK; arbitrary peak value 0.2). Scale bars, (*a–e*) 10 µm.

3.3. Optics and anatomy of the blue scales

Both the spectral properties and the structure of the blue scales differ substantially from those of the other coloured scales (figure 4). Observed with epi-illumination at high magnification, the main area of the scales reflects blue light, but locally more purplish colours emerge (figure 4*a*). In transmitted light a pale colour remains, indicating no or at least little pigmentation (figure 4*b*). The coloration hence must have a structural origin. To better understand the optical properties of scales, we therefore first performed imaging scatterometry, because ideal multilayers have specular characteristics, and therefore create a point-like scatterogram when illuminated with a narrow-aperture beam [19,25]. However, illumination of a small area (diameter approx. 13 µm) of a blue scale with a narrow-aperture white-light beam caused a scatterogram showing a rather widespread, variable light distribution (figure 4*c*). This implied that even locally the reflecting structures do not well approximate an ideal multilayer.

To assemble further information about the variable blue to purple coloration, we measured the reflectance from small areas ($5 \times 5\ \mu m^2$) of scales attached to the cuticle, as well as from the cuticle in between the scales, with the MSP (figure 4*d*). The reflectance spectra of the cuticle peaked in the blue, near 500 nm (figure 4*d*). The spectra of the blue scales were rather variable, with narrow peaks in the blue wavelength range and clear oscillations at longer wavelengths (figure 4*d*). To investigate the presence of pigment, we immersed isolated scales in water and thus measured the transmittance, which appeared to be high, only slightly deviating from 100% (figure 4*e*). Because some reflections will remain, even when the water has penetrated the scale, owing to the unequal refractive indices of water and chitin, this demonstrated that the scales contained at most a minor amount of pigment. Undoubtedly, therefore, the blue-peaking reflectance has a structural origin.

To understand the optics of the reflecting structures, we studied the anatomy of the scales via scanning electron microscopy. The blue scales appeared to be flattened tubes or sacks with a rather rumpled surface plane (figure 4*f*), which explained the non-unidirectional spatial distribution of the scatterogram (figure 4*c*). Cutting the scales showed an approximately 350 nm thickness of each of the two scale layers (figures 4*g* and 5*a*). The outer surface of scales furthermore featured on both the upper and under side a dense array of longitudinal ridges with height approximately 50 nm and spacing approximately 120 nm (figures 4*f,g* and 5*a*). The inside surfaces also featured ridges, however oriented perpendicularly to the ridges at the outside, with height approximately 30 nm and spacing approximately 140 nm. Overlain at the inside ridges were crossed filaments (hence parallel to the longitudinal outside ridges), approximately 100 nm thick and approximately 250 nm spaced apart (figures 4*g* and 5*a*; see also electronic supplementary material, figure S1). As the spacings of the ridges and filaments are too small to create diffraction colours and thus will not contribute a hue, the two flattened tube layers must play a major role in the scale coloration. We investigated that further by spectral modelling.

3.4. Spectral modelling

For modelling the spectral properties of the blue scales, we used a matrix transfer formalism for multilayers. As will be discussed below, we neglected the ridge layer at the scale inside because of its minor height compared with the other optical components (figure 5*b*). Figure 5*c* shows the refractive index profile of the general model scale (for 500 nm wavelength light). In the outside ridge layer (thickness d_r), the refractive index gradually increases from that of air, $n_a = 1.0$, to that of chitin, $n_c(500) = 1.55$. For the filament layer, we used a filling factor of 0.25, estimated from the anatomy of figure 5*a*, which then has a refractive index $n_f(500) = 1.14$.

We considered three cases, where we applied normal illumination to the model multilayer. First, we neglected both the ridge and filament layers, i.e. $d_r = d_f = 0$ nm. To obtain a blue-peaking spectrum similar as the spectra of figure 4*d*, we chose for the values of the thickness of the chitin and air layers $d_c = 380$ nm and $d_a = 160$ nm. The resulting reflectance spectrum (spectrum *a* in figure 6*a*) has three main bands, in the ultraviolet, blue and far-red (cf. Land *et al.* [17]). Minor changes in the thickness of the chitin or the air layer caused small spectral shifts in the reflectance bands (see electronic supplementary material, figure S2*a,b*). Second, adding the outside ridge layers with thickness $d_r = 50$ nm, and adjusting the chitin layer to $d_c = 355$ nm, while keeping $d_a = 160$ nm and $d_f = 0$ nm, yielded spectrum *b* of figure 6*a*, showing that except for a slight decrease in height, the reflectance bands remained almost unchanged. Finally, addition of the filament layer, with $d_f = 100$ nm and filling factor 0.25, and taking $d_r = 50$ nm, $d_c = 360$ nm, $d_a = 160$ nm, resulted in a clear, blue-peaking reflectance band with a remaining, distinctly decreased far-red band. The main effect appeared to be a distinctly narrowed blue band, and the emergence of minor side

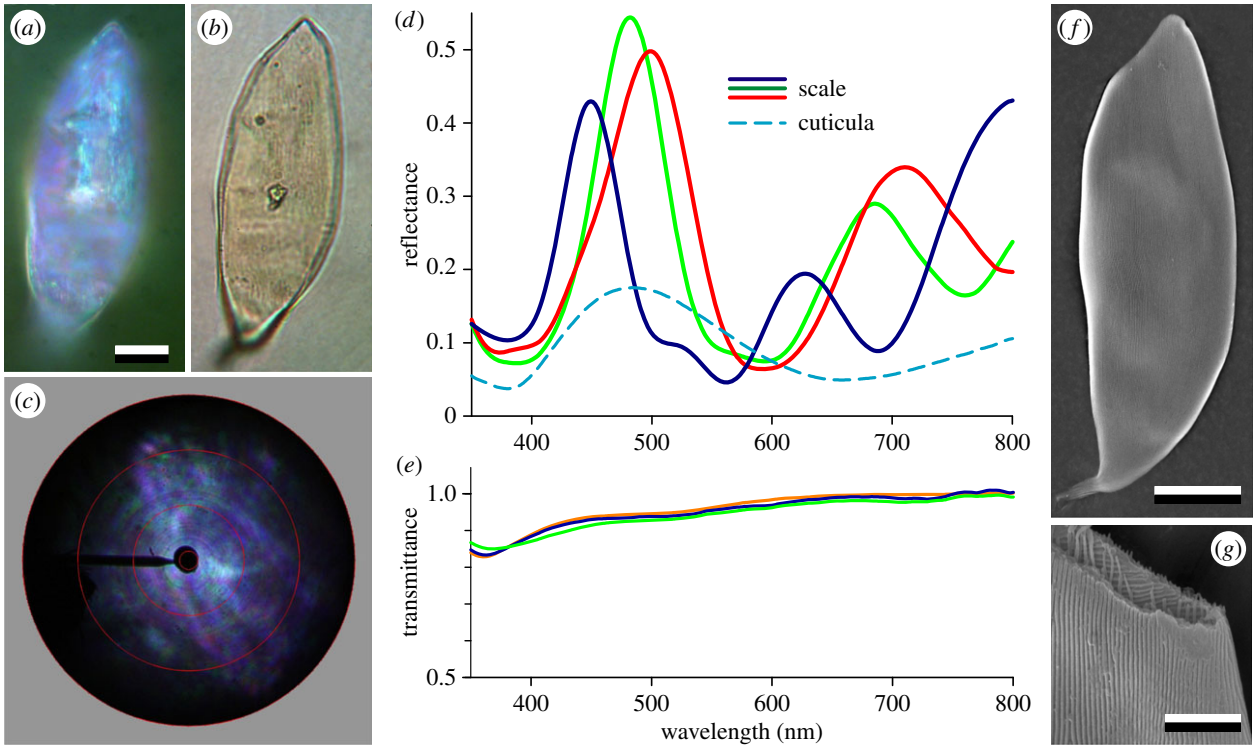

Figure 4. Optical properties of the iridescent, blue scales of *Maratus splendens*. (*a*) Epi-illumination light microscopy of a blue scale. (*b*) The same scale observed with transmitted light. (*c*) Scatterogram of a blue scale, showing somewhat wide-field reflections. (*d*) Reflectance spectra measured with a microspectrophotometer from various locations of blue scales and from the cuticula in between the scales; the size of the measurement area was 5×5 μm^2. (*e*) Transmittance spectra of a few blue scales immersed in water. (*f*) Scanning electron micrograph of a blue scale showing longitudinal ridges. (*g*) A sectioned blue scale showing an additional meshwork of ridges and filaments at the scale interior. Scale bars, (*a*,*f*) 10 μm; (*g*) 2 μm.

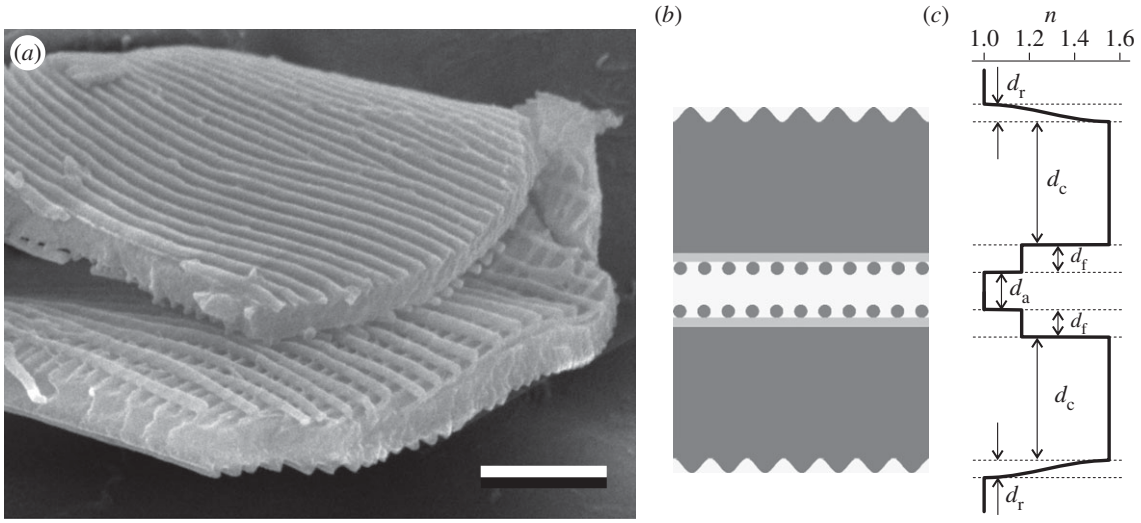

Figure 5. Blue scale profile. (*a*) Scanning electron microscopy of a sectioned scale of *Maratus splendens* showing ridge layers at the scale outside and inside, which are arranged perpendicular to each other. An array of filaments on the inside is directed parallel to the outside ridges. Scale bar, 1 μm. (*b*) Diagram of a cross-sectioned scale, consisting of two solid layers with thickness d_c with at the outside a sinusoidal ridge layer with thickness d_r. At the inner side of each solid layer, another ridge layer exists, with ridges oriented perpendicularly to those of the outer ridges. Together with a layer of filaments, which run parallel to the outer ridges, the inner ridges create an effective layer with thickness d_f. In between the two components of symmetrically organized multilayers, an air gap with thickness d_a exists. (*c*) Refractive index profile of the model scale (for light with wavelength 500 nm).

bands. Increasing the filling factor to above 0.3 caused further narrowing of the blue band, but also a decreased peak value and increased side bands (electronic supplementary material, figure S2*c*).

To investigate the iridescence properties of the blue scales, we used the last model case and applied illumination from five angles of incidence. The angle-dependence of the reflectance spectrum for unpolarized light was obtained by averaging the spectra calculated for TE- and TM-polarized light (figure 5*b*; see electronic supplementary material, figure S3). The spectra show the characteristic short-wavelength shift with increasing angle of incidence, typical for dielectric multilayers.

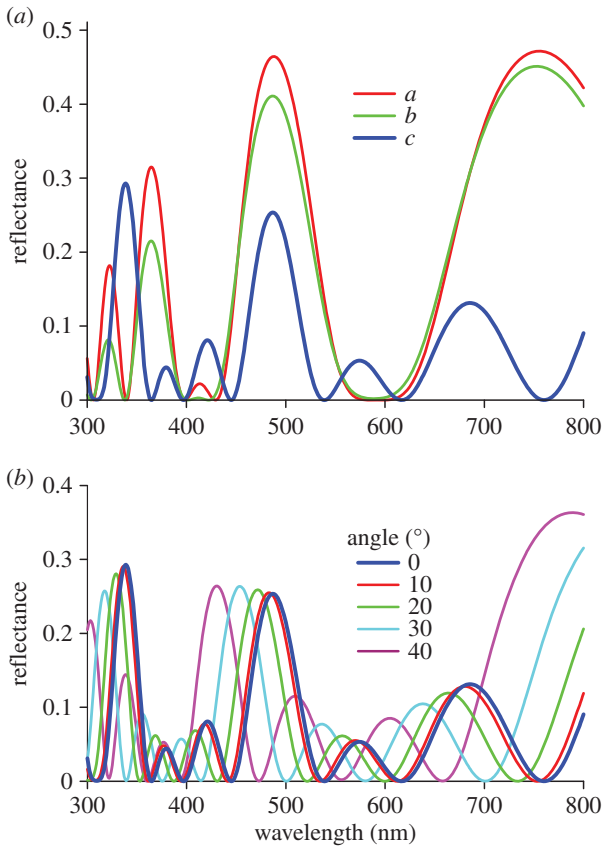

Figure 6. Reflectance spectra of model scales. (*a*) Reflectance spectra for normal illumination of three cases; *a*: the ideal case of two chitin layers, with $d_r = d_f = 0$ nm, $d_c = 380$ nm, $d_a = 160$ nm; *b*: two chitin layers with only ridges on the outside, with $d_r = 50$ nm, $d_c = 355$ nm, $d_a = 160$ nm; *c*: as *b*, but with $d_c = 360$ nm, $d_a = 160$ nm and additionally a filament layer with thickness $d_f = 100$ nm, where chitinous filaments take up a fraction 0.25 of the layer volume. (*b*) Reflectance spectra of model scale *c* illuminated from angles of incidence 0–40° in steps of 10° (mean of reflectance of TE- and TM-polarized light; see electronic supplementary material, figure S3).

4. Discussion

4.1. Coloration mechanisms of jumping spiders

Variously coloured scales cover the body of the male peacock spider *M. splendens*. The body's cuticle consists of blue-reflecting cells with a convex surface (figure 1*e*). The cuticular reflectance spectrum of figure 4*d* shows a shallow trough near 700 nm, suggesting a simple chitinous thin film of approximately 230 nm thickness (cf. [21]), but as the cuticle is mainly covered by scales, we have not further investigated the structure causing the blue colour. The white scales possibly contain 3-OH-kynurenine pigment, whereas the cream scales may have also xanthommatin and the red scales a large amount of the latter pigment. The numerous spines of the pigmented scales are responsible for their strongly diffusive scattering (figures 2 and 3).

The blue scales are transparent and thus contain no pigment (figure 4*e*). Their structure is deceptively simple, as it seems to be essentially a flattened tube and thus should act as two chitin layers with an air layer between them, similar to the scales of the male jumping spider *C. umbratica* [17]. However, modelled spectra for such a multilayer do not conform to the experimentally obtained reflectance spectra (figures 4*d* versus 6*a*, curve *a*). This cannot be owing to the ridge layer at the scale outside, because that has a minor reflectance-reducing effect owing to its relatively low thickness of approximately 50 nm (figure 6*a*, curve *b*). Increasing the ridge height from $d_r = 50$ nm to above 100 nm resulted in considerably reduced reflectance peaks, however. The ridge layer then starts to become an effective refractive index matching device (i.e. an anti-reflection coating), similar to that of the corneal nipple array of moths and butterflies [26].

Distinctly oscillating reflectance spectra, like the measured ones, are obtained with model calculations where the inside filaments are included as a layer with a refractive index intermediate between air and chitin (figure 6*a*, curve *c*). The reflectance peak values appeared to be quite sensitive to the value of the filament layer's filling factor, which is proportional to the spacing of the filaments (electronic supplementary material, figure S2*c*). Increasing the filling factor caused narrowing of the blue reflectance band, but also decreased the peak value as well as enhanced the sidebands. A filling factor of approximately 0.25 seems to be optimal to achieve a pronounced, narrow reflectance band while at the same time keeping the sidebands at minor intensities.

The colour of the blue scales varies over the scale area and the reflectance spectra measured at various areas accordingly differ distinctly (figure 4*a*,*d*), indicating a considerable variation in the anatomical parameters. The undulating surface will be the main cause for the spatial spread in the scatterogram and possibly has important spectral effects (figure 4*c*). As in any multilayer structure, the reflectance spectrum of the blue scales shifts to shorter wavelengths when the angle of incidence of the illumination increases (figure 6*b*) [20,22]. The reflectance spectrum then depends strongly on the polarization of the light beam (electronic supplementary material, figure S3). With normal illumination, this dependence is absent for the model multilayers, assumed to be homogeneous. However, the longitudinally arranged ridges and filaments will create form birefringence, which will result in different reflectance spectra for polarized light parallel or perpendicular to the structures, even with normally incident light. Indeed, scales isolated from the opisthosoma and observed with an epi-illumination microscope using crossed polarizer and analyser showed a distinct polarization dependence of the blue scales but not of the cream and red scales (electronic supplementary material, figure S4). Whether polarization-dependent reflections might be important for spider communication seems to be unlikely, however, as it would require scales to be arranged in a more orderly way than observed in this species.

As noted above, the anatomy of the blue scales of *M. splendens* appears to have a quite similar design to that of the ultraviolet and green–orange reflecting scales of *C. umbratica*, investigated in detail by Land *et al.* [17]. The reflectance spectra of these scales could be well understood by assuming two smooth chitin layers with an air gap in between, which was concluded from light microscopic sections and transmission electron micrographs. However, the reflectance spectra of the *C. umbratica* scales differ distinctly from the spectra of the blue *M. splendens* scales, in both the spectral location and shape of the peaks. In our calculations, we found that the ridge layer at the scales' outside had a minor spectral effect. The effect of the ridges at the scales' inside is even less because of the smaller ridge height. However, the added filament layer at the scales' inside had a major spectral effect, and we therefore conclude that it causes the distinct difference in spectral

properties of the *M. splendens* scales from those of the scales of *C. umbratica*. The filament layer appears to be a novel invention of the peacock spider to subtly adjust the colour of the iridescent blue scales.

4.2. Spider display and colour vision

Male *Maratus* spiders are extremely visual animals [1,2,27], see https://www.youtube.com/watch?v=1355RCne5w0, and thus it is interesting to consider how the different scale colours are detected by the visual system of spiders. Electrophysiological recordings from the principal eyes of other jumping spider species, *Phidippus reqius* and *Plexippus* sp., demonstrated the presence of at least two classes of spectral photoreceptors, with peak sensitivities in the ultraviolet (approx. 360 nm) and green (approx. 520 nm) [28,29]. Recently, Zurek *et al*. investigated the principal eyes of the jumping spider *Habronattus pyrrithrix*, using spectrophotometry to characterize the absorbance spectra of the visual pigments in retinal sections [30]. In agreement with the previous studies, two photopigments were identified, absorbing maximally at approximately 377 and 530 nm, but in addition a ruby-red photostable pigment was found, with apparent function to act as a spectral long-pass filter for the underlying green receptors. This spectral filter will change the green receptors into narrow-band red receptors, much as occurs in butterflies [31,32], thus creating a trichromatic colour vision system.

Whether the same spectral receptors are present in the eyes of *M. splendens* is unknown, but given the highly coloured bodies of this and related jumping spiders it seems rather likely that also *M. splendens* has a rich spectral set of photoreceptors. Notably the red scales with reflectances well above 600 nm are good candidates for detection by a red receptor (figure 2*e*). The blue scales with their violet-blue peaking reflectance spectra create a puzzle, however. They have a main reflectance band in the blue wavelength range with additional bands in the ultraviolet and red. The distinct blue–red pattern of the male's opisthosoma produces strong colour contrast for the human eye. Whether such a contrast is perceived by *M. splendens* depends on the visual sensitivities of these animals, and particularly whether they have blue and red receptors (which probably is the case; N. Morehouse 2016, personal communication). Future research should resolve this enigma.

Authors' contributions. D.G.S. conceived the study, carried out experiments and modelling and drafted the manuscript; J.C.O. provided specimens; B.D.W. performed experiments, participated in modelling and the design of the study and helped draft the manuscript. All authors gave final approval for publication.

Competing interests. We declare we have no competing interests.

Funding. This research was partly supported through the Air Force Office of Scientific Research/European Office of Aerospace Research and Development AFOSR/EOARD (grant no. FA9550-15-1-0068 to D.G.S.) and by the National Centre of Competence in Research 'bio-inspired materials' and the Adolphe Merkle Foundation (to B.D.W.).

Acknowledgement. Hein Leertouwer provided excellent technical assistance. Critical reading of the paper by Drs Michael Land and Nate Morehouse is gratefully acknowledged.

References

1. Hill DE, Otto JC. 2011 Visual display by male *Maratus pavonis* (Dunn 1947) and *Maratus splendens* (Rainbow 1896)(Araneae: Salticidae: Euophryinae). *Peckhamia* **89**, 1–41.
2. Girard MB, Kasumovic MM, Elias DO. 2011 Multimodal courtship in the peacock spider, *Maratus volans* (OP-Cambridge, 1874). *PLoS ONE* **6**, e25390. (doi:10.1371/journal.pone.0025390)
3. Otto JC, Hill DE. 2012 Notes on *Maratus* Karsch 1878 and related jumping spiders from Australia, with five new species (Araneae: Salticidae: Euophryinae). *Peckhamia* **103**, 1–81.
4. Foelix RF, Erb B, Hill DE. 2013 Structural colors in spiders. In *Spider ecophysiology* (ed. W Nentwig), pp. 333–347. Berlin, Germany: Springer.
5. Girard MB, Endler JA. 2014 Peacock spiders. *Curr. Biol*. **24**, R588–R590. (doi:10.1016/j.cub.2014.05.026)
6. Insausti TC, Casas J. 2008 The functional morphology of color changing in a spider: development of ommochrome pigment granules. *J. Exp. Biol*. **211**, 780–789. (doi:10.1242/jeb.014043)
7. Holl A. 1987 Coloration and chromes. In *Ecophysiology of spiders* (ed. W Nentwig), pp. 16–25. Berlin, Germany: Springer.
8. Riou M, Christidès J. 2010 Cryptic color change in a crab spider (*Misumena vatia*): identification and quantification of precursors and ommochrome pigments by HPLC. *J. Chem. Ecol*. **36**, 412–423. (doi:10.1007/s10886-010-9765-7)
9. Seligy VL. 1972 Ommochrome pigments of spiders. *Comp. Biochem. Physiol. A* **42**, 699–709. (doi:10.1016/0300-9629(72)90448-3)
10. Hsiung BK, Blackledge TA, Shawkey MD. 2015 Spiders do have melanin after all. *J. Exp. Biol*. **218**, 3632–3635. (doi:10.1242/jeb.128801)
11. Hill DE. 1979 The scales of salticid spiders. *Zool. J. Linn. Soc*. **65**, 193–218. (doi:10.1111/j.1096-3642.1979.tb01091.x)
12. Townsend VR, Felgenhauer BE. 1999 Ultrastructure of the cuticular scales of lynx spiders (Araneae, Oxyopidae) and jumping spiders (Araneae, Salticidae). *J. Morphol*. **240**, 77–92. (doi:10.1002/(SICI)1097-4687(199904)240:1<77::AID-JMOR6>3.0.CO;2-P)
13. Parker AR, Hegedus Z. 2003 Diffractive optics in spiders. *J. Opt. A* **5**, S111. (doi:10.1088/1464-4258/5/4/364)
14. Ingram A, Ball A, Parker A, Deparis O, Boulenguez J, Berthier S. 2009 Characterization of the green iridescence on the chelicerae of the tube web spider, *Segestria florentina* (Rossi 1790) (Araneae, Segestriidae). *J. Arachnol*. **37**, 68–71. (doi:10.1636/SH07-87.1)
15. Ingram A, Deparis O, Boulenguez J, Kennaway G, Berthier S, Parker A. 2011 Structural origin of the green iridescence on the chelicerae of the red-backed jumping spider, *Phidippus johnsoni* (Salticidae: Araneae). *Arthropod Struct. Dev*. **40**, 21–25. (doi:10.1016/j.asd.2010.07.006)
16. Hsiung B, Deheyn DD, Shawkey MD, Blackledge TA. 2015 Blue reflectance in tarantulas is evolutionarily conserved despite nanostructural diversity. *Sci. Adv*. **1**, e1500709. (doi:10.1126/sciadv.1500709)
17. Land MF, Horwood J, Lim ML, Li D. 2007 Optics of the ultraviolet reflecting scales of a jumping spider. *Proc. R. Soc. B* **274**, 1583–1589. (doi:10.1098/rspb.2007.0328)
18. Lim ML, Li D. 2013 UV-green iridescence predicts male quality during jumping spider contests. *PLoS ONE* **8**, e59774. (doi:10.1371/journal.pone.0059774)
19. Stavenga DG, Leertouwer HL, Pirih P, Wehling MF. 2009 Imaging scatterometry of butterfly wing scales. *Opt. Express* **17**, 193–202. (doi:10.1364/OE.17.000193)
20. Yeh P. 2005 *Optical waves in layered media*. Hoboken, NJ: Wiley-Interscience.
21. Stavenga DG. 2014 Thin film and multilayer optics cause structural colors of many insects and birds. *Mater. Today Proc*. **1**, 109–121. (doi:10.1016/j.matpr.2014.09.007)
22. Stavenga DG, Wilts BD, Leertouwer HL, Hariyama T. 2011 Polarized iridescence of the multilayered elytra of the Japanese jewel beetle, *Chrysochroa fulgidissima*. *Phil. Trans. R. Soc. B* **366**, 709–723. (doi:10.1098/rstb.2010.0197)

23. Leertouwer HL, Wilts BD, Stavenga DG. 2011 Refractive index and dispersion of butterfly scale chitin and bird feather keratin measured by interference microscopy. *Opt. Express* **19**, 24 061–24 066. (doi:10.1364/OE.19.024061)
24. Stavenga DG, Leertouwer HL, Wilts BD. 2014 Coloration principles of nymphaline butterflies: thin films, melanin, ommochromes and wing scale stacking. *J. Exp. Biol*. **217**, 2171–2180. (doi:10.1242/jeb.098673)
25. Wilts BD, Michielsen K, De Raedt H, Stavenga DG. 2014 Sparkling feather reflections of a bird-of-paradise explained by finite-difference time-domain modeling. *Proc. Natl Acad. Sci. USA* **111**, 4363–4368. (doi:10.1073/pnas.1323611111)
26. Stavenga DG, Foletti S, Palasantzas G, Arikawa K. 2006 Light on the moth-eye corneal nipple array of butterflies. *Proc. R. Soc. B* **273**, 661–667. (doi:10.1098/rspb.2005.3369)
27. Otto JC, Hill DE. 2014 Description of a new peacock spider from Cape Le Grand, Western Australia, with observations on display by males and females and comparative notes on the related *Maratus volans* (Araneae: Salticidae: Euophryinae: Maratus). *Peckhamia* **114**, 1–38.
28. De Voe RD. 1975 Ultraviolet and green receptors in principal eyes of jumping spiders. *J. Gen. Physiol*. **66**, 193–207. (doi:10.1085/jgp.66.2.193)
29. Blest A, Hardie R, McIntyre P, Williams D. 1981 The spectral sensitivities of identified receptors and the function of retinal tiering in the principal eyes of a jumping spider. *J. Comp. Physiol*. **145**, 227–239. (doi:10.1007/BF00605035)
30. Zurek DB, Cronin TW, Taylor LA, Byrne K, Sullivan ML, Morehouse NI. 2015 Spectral filtering enables trichromatic vision in colorful jumping spiders. *Curr. Biol*. **25**, R403–R404. (doi:10.1016/j.cub.2015.03.033)
31. Wakakuwa M, Stavenga DG, Kurasawa M, Arikawa K. 2004 A unique visual pigment expressed in green, red, and deep-red receptors in the eye of the small white butterfly, *Pieris rapae crucivora*. *J. Exp. Biol*. **207**, 2803–2810. (doi:10.1242/jeb.01078)
32. Stavenga DG, Arikawa K. 2011 Photoreceptor spectral sensitivities of the small white butterfly *Pieris rapae crucivora* interpreted with optical modeling. *J. Comp. Physiol. A* **197**, 373–385. (doi:10.1007/s00359-010-0622-5)